

## Metabolic Fate of Hallucinogenic NBOMes

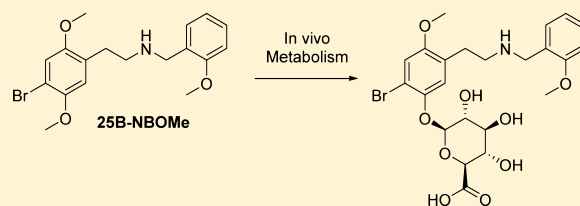
Sebastian Leth-Petersen,<sup>†,‡</sup> Charlotte Gabel-Jensen,<sup>‡,‡</sup> Nic Gillings,<sup>§</sup> Szabolcs Lehel,<sup>§</sup> Hanne D. Hansen,<sup>||</sup> Gitte M. Knudsen,<sup>||</sup> and Jesper L. Kristensen<sup>\*,†</sup>

<sup>†</sup>Department of Drug Design and Pharmacology and <sup>‡</sup>Department of Pharmacy, University of Copenhagen, DK-2100 Copenhagen, Denmark

<sup>§</sup>PET and Cyclotron Unit and <sup>||</sup>Neurobiology Research Unit and Center for Integrated Molecular Brain Imaging, Copenhagen University Hospital, DK-2100 Copenhagen, Denmark

### S Supporting Information

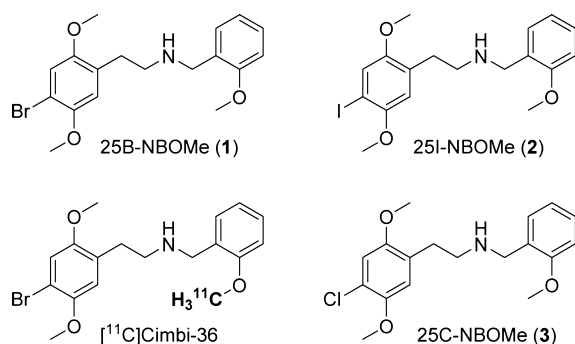
**ABSTRACT:** 2,5-Dimethoxy-*N*-benzylphenethylamines (NBOMes) are very potent 5-HT<sub>2A</sub>R agonists. Illicit use of these psychedelic compounds has emerged in recent years, and several fatalities have been linked to their recreational use. In its [<sup>11</sup>C]-labeled form, one NBOMe (25B-NBOMe) was recently developed as a PET-ligand for clinical investigations of 5HT<sub>2A</sub>R ([<sup>11</sup>C]Cimbi-36). Herein, we have identified the phase I and phase II metabolites of 25B-NBOMe in pigs as well as in humans. We find that the primary route of metabolism is 5'-demethylation, followed by conjugation to glucuronic acid. Carbon-11 labeling of 25B-NBOMe in three different positions followed by in vivo evaluation in pigs and humans corroborated these findings.



## INTRODUCTION

Since their discovery by Ralph Heim in 2003,<sup>1</sup> the 2,5-dimethoxy-*N*-benzylphenethylamines (NBOMes; Chart 1)

**Chart 1. Representative Examples from the NBOMe Class of Hallucinogens<sup>a</sup>**



<sup>a</sup>Shown are 25B-NBOMe/CIMBI-36 (1), 25I-NBOMe (2), and 25C-NBOMe (3). In its [<sup>11</sup>C]-labeled form, 1 is currently used as a PET tracer to map 5-HT<sub>2A</sub>R in humans under the designation [<sup>11</sup>C]Cimbi-36.

have attracted considerable attention from the scientific community as tools to investigate the pharmacology<sup>2–5</sup> and localization in the brain<sup>6,7</sup> of serotonin 2A receptors (5-HT<sub>2A</sub>R). The NBOMes were recently proposed to undergo extensive first-pass metabolism by the liver due to their high intrinsic clearance.<sup>8</sup> Additionally, recent reports detail severe and in some cases fatal toxicity, related to widespread illicit use of several NBOMes due to their hallucinogenic effects, which are similar to those of LSD.<sup>9–12</sup> The ability of 1, 2, and 3

(Chart 1) to precipitate severe symptoms of rhabdomyolysis in some individuals has led to their placement as schedule one drugs by the DEA in 2013. This apparent toxicity is puzzling in light of the compounds high selectivity for 5-HT<sub>2R</sub> coupled with the low toxicity of known nonselective 5-HT<sub>2R</sub> agonists such as psilocybin, mescaline, and LSD.<sup>13–15</sup> These observations led us to hypothesize that the unpredictable toxicity of NBOMes may be idiosyncratic in nature and caused by the formation of toxic metabolites. Our previous pharmacokinetic studies on the NBOMe class included screening of several closely related structural analogues, including primary phenethylamines such as mescaline and 2C-B that, in contrast to their NBOMe congeners, were very stable to human liver microsomes. Thus, we wanted to identify the metabolite(s) of NBOMe to be able to address its toxic potential.

1 (Chart 1) has been shown to be a highly efficacious and selective 5-HT<sub>2R</sub> agonist and is currently being used in its [<sup>11</sup>C]-labeled form as a PET tracer in humans.<sup>16</sup> Taking advantage of its authorized use in humans as a PET ligand (where it is given in doses < 2 μg), we embarked on a detailed investigation of the metabolic fate of 1.

## METHODS

The identification of the metabolite(s) of 1 was approached using the following techniques: In vitro degradation was evaluated via incubation with porcine and human liver microsomes. The identities of the produced phase I metabolites were identified via LC-MS and by comparison with authentic samples that were synthesized as described in the Supporting Information. Subsequently, the in vivo metabolism in pigs was investigated via injection of a pharmacological dose of 1

**Received:** October 29, 2015

**Published:** December 15, 2015

followed by LC-MS/MS analysis of blood samples to identify phase II metabolites. Structural assignment was again verified by comparison with authentic samples synthesized as detailed in the [Supporting Information](#). Finally,  $^{11}\text{C}$  labeling of **1** in various positions and administering these  $^{11}\text{C}$ -ligands to pigs and humans, followed by HPLC analysis of blood samples using a radiodetector, corroborated our structural assignment.

## RESULTS AND DISCUSSION

First, **1** was incubated with human liver microsomes (HLMs) and samples were analyzed by LC-MS. All compounds with a bromine moiety, identified by spectra displaying the typical isotopic pattern of bromine ( $^{79}\text{Br}$  (50.7%) and  $^{81}\text{Br}$  (49.3%)), were assigned as metabolites of **1** and initially designated as M1, M2, etc. The most abundant metabolites were three products with  $m/z = 366.072$  (i.e., three demethylated metabolites; [Figure 1](#), M10, M12, and M14) and one with

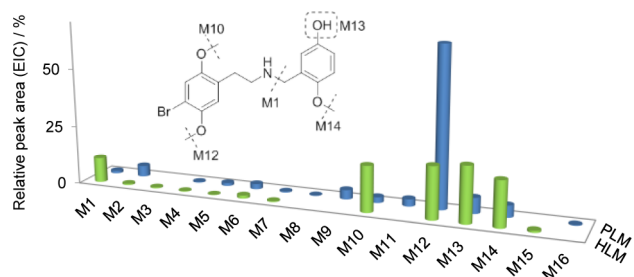


**Figure 1.** Relative abundance of phase I metabolites from degradation studies with porcine liver microsomes (PLMs) and human liver microsomes (HLMs).

$m/z = 396.084$  (i.e., hydroxylation; [Figure 2](#), M13). Although it was less abundant, N-debenzylation was also observed ([Figure 1](#), M1; see the [Supporting Information](#) for full details).

Since we had access to *in vivo* studies in pigs, **1** was also incubated with pig liver microsomes (PLMs) in order to compare the results with the HLM data. Qualitatively, the metabolites in human and pig liver microsomes were similar, but the relative quantity of the metabolites differed, with M12 being the major metabolite in the PLM experiments ([Figure 1](#)). All of the detected metabolites were further analyzed by LC-MS/MS to gain additional structural information. Because it is more sensitive, LC-MS/MS analysis resulted in the detection of metabolites that were not observed by LC-MS analysis. Table S1 in the [Supporting Information](#) summarizes the accurate mass and fragment ion data for all metabolites detected in PLMs and HLMs along with proposed metabolite structures.

In order to determine the *in vivo* metabolic profile in pig, 2 mg of **1** HCl was administered intravenously to a fully anesthetized female Danish landrace pig (21 kg). Blood samples were drawn over 2 h and analyzed by LC-MS/MS. In addition to the parent compound **1**, two major metabolites were detected in the plasma. The primary metabolite had an  $m/z = 542.101$ , corresponding to demethylation of **1** followed by conjugation to glucuronic acid, a metabolic pathway often seen for anisole derivatives.

In order to unequivocally establish the identity of this metabolite, we synthesized authentic samples of M10, M12, and M14 and their corresponding glucuronides ([Figure 2](#) and [Supporting Information](#)). Upon comparison, the identity of the  $m/z = 542.101$  metabolite from the *in vivo* pig experiment was determined to be glucuronide **9**.

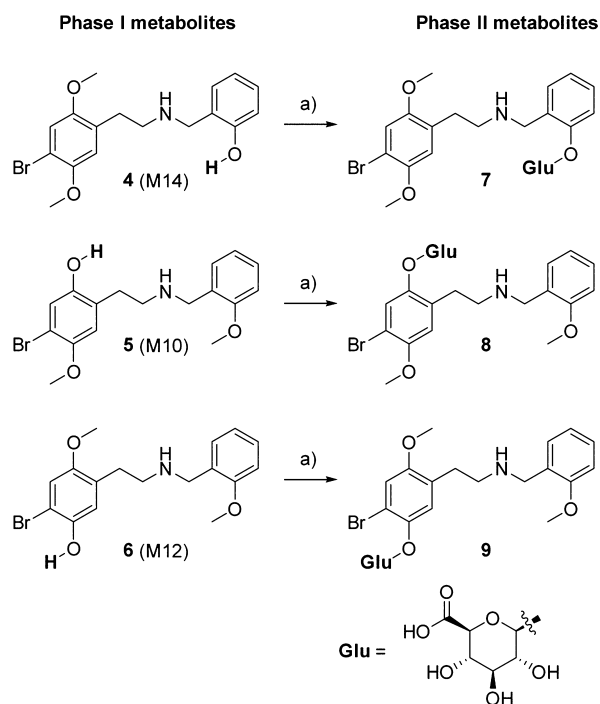


**Figure 2.** Structures of the demethylated phase I and derived glucuronated phase II metabolites of **1**. Reagents and conditions: (a) (1) 1,2,3,4-tetra-*O*-acetyl- $\beta$ -D-glucuronic acid methyl ester,  $\text{BF}_3$ ,  $\text{CH}_2\text{Cl}_2$ , rt; (2) KCN,  $\text{H}_2\text{O}$ , MeOH, rt. See the [Supporting Information](#) for full experimental details.

Quantification of **1** and its two primary metabolites in the pig (**6** and **9**) showed very fast clearance of the parent compound from plasma ([Figure 3](#)). Both metabolic steps (demethylation

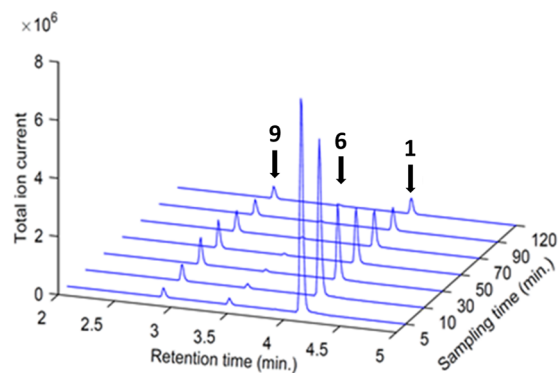


**Figure 3.** LC-MS/MS chromatograms of pig plasma samples showing the relative abundance of **1**, **6**, and **9** over time after IV injection of **1**.

and glucuronidation) are very fast, with only minute levels of intermediate phenol **6** present at any time point, whereas glucuronide **9** is eliminated much slower from plasma. At the 30 min mark, there is more than twice as much glucuronide **9** present in plasma as there is **1** ([Supporting Information](#) and [Figure 2](#)).

When used as a PET tracer in pigs and humans, **1** produces a hitherto unidentified radioactive metabolite that does not cross the blood–brain barrier in the pig.<sup>6</sup> On the basis of the data presented above, we hypothesized that this metabolite is [ $^{11}\text{C}$ ]**9**. To confirm this assumption, we produced [ $^{11}\text{C}$ ]-labeled **1**, where the label is placed sequentially on all three possible methoxy positions via alkylation of suitable precursors with

either  $[^{11}\text{C}]\text{CH}_3\text{I}$  or  $[^{11}\text{C}]\text{CH}_3\text{OTf}$  (see the [Supporting Information](#) for details). If our structural assignment is correct, then two of them (**11** and **12**) should lead to the same radioactive metabolite, whereas the last (**13**) should not ([Figure 4](#)). Compound **14**, which is the presumed phase I metabolite of

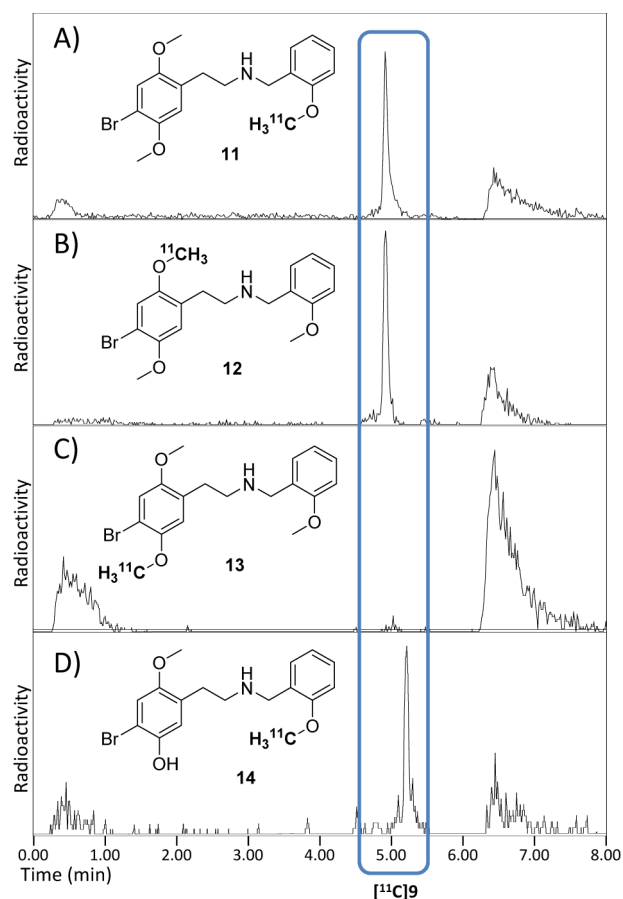


**Figure 4.** HPLC radiochromatograms of plasma samples from PET experiments in pigs with (A) **11**, (B) **12**, (C) **13**, and (D) **14**. The blue box highlights the presence or absence of the  $[^{11}\text{C}]$ -labeled glucuronide  $[^{11}\text{C}]$ 9.

**1**, was also included in the study as this should lead to the same phase II metabolite. All of these  $[^{11}\text{C}]$ -labeled ligands were injected into Danish landrace pigs in separate experiments, and blood samples were collected and analyzed by HPLC using a radiodetector.

As seen in [Figure 4A,B](#), **11** and **12** lead to the formation of the same radioactive metabolite, which has a retention time identical to that of **9**. When the label is moved to the last methoxy group ([Figure 4C](#)),  $[^{11}\text{C}]$ 9 is no longer produced. That is, even though **9** is still formed, it is no longer detectable because it is not  $[^{11}\text{C}]$ -labeled. Furthermore, injection of **14** ([Figure 4D](#)) leads to the same radioactive metabolite as that in [Figure 4A,B](#), confirming that we have established the identity of the major metabolite as  $[^{11}\text{C}]$ 9.

When radioactive metabolites of a CNS PET tracer are produced in significant amounts and cross the blood–brain barrier, this generates problems with correct quantification. Thus, a head-to-head comparison in humans of  $[^{11}\text{C}]$ Cimbi-36 labeled at two different positions (**11** and **13**) was initiated, and the conclusions from that study will be published elsewhere in due course, but some preliminary data on the metabolism will

be provided here. On the basis of the PLM and HLM data presented in [Figure 2](#), one might expect to see several abundant metabolites in vivo in humans compared to those in pigs, but we found that the metabolism in humans follows the same pathway as that in the pig. Furthermore, the rate of metabolism at tracer doses of **11** in humans is comparable to that in pigs.<sup>7</sup> In [Figure 5](#), the combined data from three head-to-head

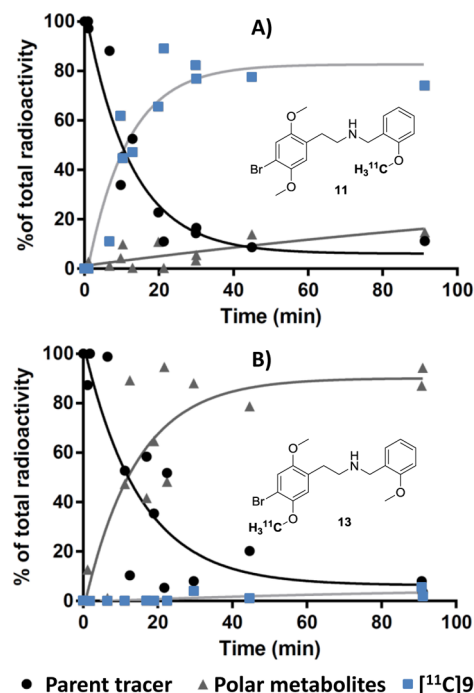


**Figure 5.** Two graphs show the collected data from three head-to-head comparisons in humans of **11** and **13**. In (A) the same metabolite as that found in the pig experiments accumulates over time, whereas in (B) this radiolabeled metabolite is absent (analogous to [Figure 4C](#)). Polar metabolites refer to fast eluting metabolites appearing within the first 2 min in the HPLC chromatograms from the plasma samples (see the [Supporting Information](#) for details).

comparisons of **11** and **13** in humans is presented. **11** leads to the formation of the same major metabolite as that in pigs:  $[^{11}\text{C}]$ 9. Switching the site of labeling (**11** to **13**) leads to the disappearance of this metabolite, in analogy to the data from the pig experiments. Accordingly, we suggest that the major metabolite of **1** in humans is **9**. The same hitherto unidentified radioactive metabolite is also present in plasma from human investigations with **11**, which confirms that 5'-demethylation followed by glucuronic acid conjugation is also the primary route of metabolism of **1** in humans.

We previously conducted a tracer development study, where several structurally similar  $[^{11}\text{C}]$ -labeled analogues of **1** were investigated as PET ligands, including **2** and **3**. Upon inspection of the radiochromatograms, a large peak at approximately the same retention time as that of glucuronide **9** is present in all other NBOMe-derived ligands.<sup>6</sup> Therefore, we speculate that the closest analogues of **1** (including **2** and **3**) are transformed in a similar fashion via 5'-demethylation followed by glucuronic acid conjugation ([Figure 6](#)).

This hypothesis is consistent with recently published MS analysis of 25I-NBOMe (**2**) and 25C-NBOMe (**3**) in human urine.<sup>17–19</sup> With this in mind, we suggest that a glucuronated metabolite is more abundant in plasma than the NBOMe itself

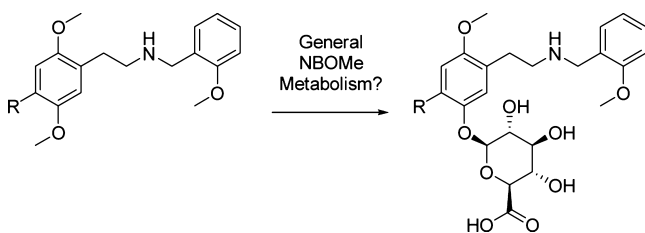


**Figure 6.** Proposed general metabolic fate of the NBOMe class of hallucinogens.

following ingestion of pharmacological doses and that these metabolites are responsible for the toxic effect of NBOMes (Figure 6). Furthermore, they are prime candidates as markers for NBOMe intoxication within forensic science. In particular, 25I-NBOMe (2) has seen widespread illicit use, and we suggest that the corresponding 5'-glucuronide will be a good marker for this compound given the apparent stability of these metabolites in vivo.

## CONCLUSIONS

We have identified and synthesized the major metabolite of hallucinogenic and toxic 25B-NBOMe (1).

## ASSOCIATED CONTENT

### Supporting Information

The Supporting Information is available free of charge on the ACS Publications website at DOI: 10.1021/acs.chemrestox.5b00450.

Synthesis details, characterization, metabolism, LC-MS/MS analysis, radio labeling, and animal experiments (PDF)

## AUTHOR INFORMATION

### Corresponding Author

\*E-mail: [jesper.kristensen@sund.ku.dk](mailto:jesper.kristensen@sund.ku.dk). Phone: (+45) 35336487.

### Author Contributions

<sup>†</sup>S.L.-P. and C.G.-J. contributed equally to this work.

### Funding

Generous support from the Lundbeck foundation is gratefully acknowledged.

### Notes

The authors declare no competing financial interest.

## ACKNOWLEDGMENTS

Anders Ettrup is acknowledged for help with the handling of the pigs and the blood samples, Anette Johansen, for coordinating the clinical scannings, Agnete Dyssegaard, for help with the radioactive metabolite analysis, and Lisbeth Kværnø, for help with the synthesis of the glucuronides.

## ABBREVIATIONS

PLM, porcine liver microsomes; HLM, human liver microsomes; CNS, central nervous system; PET, positron emission tomography; DEA, Drug Enforcement Administration

## REFERENCES

(1) Heim, R. (2004) *Synthese und Pharmakologie Potenter 5-HT<sub>2A</sub>-Rezeptoragonisten mit N-2-Methoxybenzyl-Partialstruktur*, Ph.D. Thesis, Freie Universität Berlin.

(2) Juncosa, J. I., Jr., Hansen, M., Bonner, L. A., Cueva, J. P., Maglathlin, R., McCorvy, J. D., Marona-Lewicka, D., Lill, M. A., and Nichols, D. E. (2013) Extensive rigid analogue design maps the binding conformation of potent N-benzylphenethylamine 5-HT<sub>2A</sub> serotonin receptor agonist ligands. *ACS Chem. Neurosci.* 4, 96–109.

(3) Hansen, M., Phonekeo, K., Paine, J. S., Leth-Petersen, S., Begtrup, M., Brauner-Osborne, H., and Kristensen, J. L. (2014) Synthesis and structure-activity relationships of N-benzyl phenethylamines as 5-HT<sub>2A/2C</sub> agonists. *ACS Chem. Neurosci.* 5, 243–249.

(4) Braden, M. R., Parrish, J. C., Naylor, J. C., and Nichols, D. E. (2006) Molecular interaction of serotonin 5-HT<sub>2A</sub> receptor residues Phe339(6.51) and Phe340(6.52) with superpotent N-benzyl phenethylamine agonists. *Mol. Pharmacol.* 70, 1956–1964.

(5) Fantegrossi, W. E., Gray, B. W., Bailey, J. M., Smith, D. A., Hansen, M., and Kristensen, J. L. (2015) Hallucinogen-like effects of 2-([2-(4-cyano-2,5-dimethoxyphenyl) ethylamino]methyl)phenol (25CN-NBOH), a novel N-benzylphenethylamine with 100-fold selectivity for 5-HT receptors, in mice. *Psychopharmacology* 232, 1039–1047.

(6) Ettrup, A., Hansen, M., Santini, M. A., Paine, J., Gillings, N., Palner, M., Lehel, S., Herth, M. M., Madsen, J., Kristensen, J., Begtrup, M., and Knudsen, G. M. (2011) Radiosynthesis and in vivo evaluation of a series of substituted <sup>11</sup>C-phenethylamines as 5-HT (2A) agonist PET tracers. *Eur. J. Nucl. Med. Mol. Imaging* 38, 681–693.

(7) Finnema, S. J., Stepanov, V., Ettrup, A., Nakao, R., Amini, N., Svedberg, M., Lehmann, C., Hansen, M., Knudsen, G. M., and Halldin, C. (2014) Characterization of [(11)C]Cimbi-36 as an agonist PET radioligand for the 5-HT(2A) and 5-HT(2C) receptors in the nonhuman primate brain. *NeuroImage* 84, 342–353.

(8) Leth-Petersen, S., Bundgaard, C., Hansen, M., Carnerup, M. A., Kehler, J., and Kristensen, J. L. (2014) Correlating the metabolic stability of psychedelic 5-HT(2A) agonists with anecdotal reports of human oral bioavailability. *Neurochem. Res.* 39, 2018–2023.

(9) Hill, S. L., Doris, T., Gurung, S., Katebe, S., Lomas, A., Dunn, M., Blain, P., and Thomas, S. H. L. (2013) Severe clinical toxicity associated with analytically confirmed recreational use of 25I-NBOMe: case series. *Clin. Toxicol.* 51, 487–492.

(10) Poklis, J. L., Nanco, C. R., Troendle, M. M., Wolf, C. E., and Poklis, A. (2014) Determination of 4-bromo-2,5-dimethoxy-N-[(2-methoxyphenyl)methyl]-benzeneethanamine (25B-NBOMe) in serum and urine by high performance liquid chromatography with tandem mass spectrometry in a case of severe intoxication. *Drug Test. Anal.* 6, 764–769.

(11) Tang, M. H. Y., Ching, C. K., Tsui, M. S. H., Chu, F. K. C., and Mak, T. W. L. (2014) Two cases of severe intoxication associated with analytically confirmed use of the novel psychoactive substances 25B-NBOMe and 25C-NBOMe. *Clin. Toxicol.* 52, 561–565.

(12) Lawn, W., Barratt, M., Williams, M., Horne, A., and Winstock, A. (2014) The NBOMe hallucinogenic drug series: Patterns of use, characteristics of users and self-reported effects in a large international sample. *J. Psychopharmacol.* 28, 780–788.

(13) Studerus, E., Komater, M., Hasler, F., and Vollenweider, F. X. (2011) Acute, subacute and long-term subjective effects of psilocybin in healthy humans: a pooled analysis of experimental studies. *J. Psychopharmacol.* 25, 1434–1452.

(14) Krebs, T. S., and Johansen, P. O. (2013) Psychedelics and mental health: a population study. *PLoS One* 8, e63972.

(15) Schmid, Y., Enzler, F., Gasser, P., Grouzmann, E., Preller, K. H., Vollenweider, F. X., Brenneisen, R., Müller, F., Borgwardt, S., and Liechti, M. E. (2015) Acute effects of LSD in healthy subjects. *Biol. Psychiatry* 78, 544–553.

(16) Ettrup, A., da Cunha-Bang, S., McMahon, B., Lehel, S., Dyssegaard, A., Skibsted, A. W., Jorgensen, L. M., Hansen, M., Baandrup, A. O., Bache, S., Svarer, C., Kristensen, J. L., Gillings, N., Madsen, J., and Knudsen, G. M. (2014) Serotonin 2A receptor agonist binding in the human brain with [<sup>11</sup>C]Cimbi-36. *J. Cereb. Blood Flow Metab.* 34, 1188–1196.

(17) Caspar, A., Helfer, A., Michely, J., Auwärter, V., Brandt, S., Meyer, M., and Maurer, H. (2015) Studies on the metabolism and



toxicological detection of the new psychoactive designer drug 2-(4-iodo-2,5-dimethoxyphenyl)-N-[(2-methoxyphenyl)methyl]-ethanamine (25I-NBOMe) in human and rat urine using GC-MS, LC-MSn, and LC-HR-MS/MS. *Anal. Bioanal. Chem.* 407, 6697–6719.

(18) Poklis, J. L., Dempsey, S. K., Liu, K., Ritter, J. K., Wolf, C., Zhang, S., and Poklis, A. (2015) Identification of Metabolite Biomarkers of the Designer Hallucinogen 25I-NBOMe in Mouse Hepatic Microsomal Preparations and Human Urine Samples Associated with Clinical Intoxication. *J. Anal. Toxicol.* 39, 607–616.

(19) Andreasen, M. F., Telving, R., Rosendal, I., Eg, M. B., Hasselstrom, J. B., and Andersen, L. V. (2015) A fatal poisoning involving 25C-NBOMe. *Forensic Sci. Int.* 251, e1–e8.